M. Devakar*, Ankush Raje and Shubham Hande

Unsteady Flow of Couple Stress Fluid Sandwiched Between Newtonian Fluids Through a Channel

https://doi.org/10.1515/zna-2017-0434
Received December 2, 2017; accepted April 2, 2018; previously published online April 30, 2018

Abstract: The aim of this article is to study the unsteady flow of immiscible couple stress fluid sandwiched between Newtonian fluids through a horizontal channel. The fluids and plates are initially at rest. At an instant of time, a constant pressure gradient is applied along the horizontal direction to generate the flow. The time-dependent partial differential equations are solved numerically using the finite difference method. The continuity of velocities and shear stresses at the fluid-fluid interfaces has been considered. The obtained results are displayed through graphs and are discussed for various fluid parameters pertaining the flow. The volume flow rate is also obtained numerically for diverse fluid parameters and is presented through a table. It is noticed that fluid velocities increased with time and reached a steady state after a certain time level. Also, the presence of couple stresses reduced the fluid velocities. Volume flow rate increased with Reynolds number and is reduced by increase of ratio of viscosities.

Keywords: Couple Stress Fluid; Horizontal Channel; Immiscible Fluid; Unsteady Flow.

PACS: 47.60.Dx.

1 Introduction

The couple stress fluid theory initiated by Stokes [1] represents a simple generalisation of the classical Newtonian fluid theory that sustains couple stresses and the body couples. In the Newtonian fluid theory, the mechanical interaction of one part of the body on another, across a surface, is assumed to be equivalent to a force distribution only. However, in the couple stress fluid theory, the mechanical interaction is assumed to be equivalent to both force and moment distribution. The concept of couple stresses results from the study of mechanical interactions taking place across a surface and, conceptually, is not related to the kinematics of motion [2]. The striking feature of this fluid model is that, unlike the Newtonian fluid model, the stress tensor is not symmetric. The fluids consisting of rigid, randomly oriented particles suspended in a viscous medium, such as blood, lubricants containing a small amount of polymer additive, colloidal suspensions, liquid crystals and synthetic fluids, can be modelled using the couple stress fluid theory [3, 4]. In view of its simplicity and numerous applications, diverse researchers across the globe worked on couple stress fluid flows for different situations. Stokes [2] himself, in his book, has documented an extensive literature on the flows of couple stress fluids. Chaturani [5] investigated the Poiseuille flow of a couple stress fluid with applications to blood flow. Devakar and Iyengar [6] discussed the run-up flow of a couple stress fluid between parallel plates. Maiti and Misra [7] have made an investigation on peristaltic transport of couple stress fluid with some applications to hemodynamics. Hayat et al. [8] studied heat transfer in a couple stress fluid over a continuous moving surface with internal heat generation and convective boundary conditions. Devakar et al. [9] obtained analytical solutions of couple stress fluid flows with slip boundary conditions. Abbas et al. [10] discussed the hydromagnetic mixed convective two-phase flow of couple stress and viscous fluids in an inclined channel. Recently, Asad et al. [11] discussed the flow of couple stress fluid with variable thermal conductivity. Naduvinamani et al. [12, 13], Lin and Hung [14] and Lin et al. [15] have made extensive studies on the theory of hydrodynamic lubrication of journal bearings based on the couple stress fluid model. In their work, it is found that the couple stress fluid possesses better load-carrying capacity than that of the classical Newtonian fluid.

The research on the flow of non-Newtonian fluid sandwiched between Newtonian fluids is reasonably underexplored despite its applicability in blood flows, chemical engineering, crude oil extraction, etc. The blood, when flowing through small arteries, behaves as a two-fluid model with the suspension of all erythrocytes (non-Newtonian) in the core region and plasma (Newtonian) in the peripheral region [16–18]. This may be visualised in Cartesian form as the sandwiched flow of core fluid between

***Corresponding author: M. Devakar,** Department of Mathematics, Visvesvaraya National Institute of Technology, Nagpur 440010, India, E-mail: m_devakar@yahoo.co.in
Ankush Raje and Shubham Hande: Department of Mathematics, Visvesvaraya National Institute of Technology, Nagpur 440010, India, E-mail: ankush.mth@gmail.com (A. Raje), shubhamhande137@gmail.com (S. Hande)

two peripheral fluids. Aside from blood flows, there are many instances in chemical industries and geology where the modelling of the flow may be desirable using the sandwiched fluid flow model. Owing to these applications, few attempts have been made in order to study the flow of immiscible non-Newtonian fluids sandwiched between two Newtonian fluids. It is worth mentioning here that Umavathi and her team have made a remarkable contribution in the advancement of sandwiched fluid flows. Since 2005, the flow and heat transfer of a couple stress fluid sandwiched between viscous fluid layers have been studied in steady flow situations by Umavathi et al. [19], obtaining closed form solutions. The flow and heat transfer of micropolar fluid sandwiched between viscous fluid layers was discussed analytically by Umavathi et al. [20]. The flow and heat transfer of couple stress permeable fluid sandwiched between viscous fluid layers was analysed by Umavathi [21].

The studies regarding sandwiched flow situations quoted above were carried out imposing the simplifying constraint of steadiness. However, there exist situations in natural as well as artificial flows, in which it is highly desirable to consider the time evolution aspect. The study of time-dependent flows of sandwiched fluids is more realistic for understanding the aforementioned applications in biomechanics, chemical engineering and hydrology. In light of this, Umavathi et al. [22] studied unsteady flow and heat transfer of porous media sandwiched between viscous fluids, which is the only attempt to study unsteady sandwiched fluid flow.

In the present investigation, an unsteady flow of immiscible couple stress fluid sandwiched between Newtonian fluids through a horizontal channel is considered. The research area of sandwiched fluid flows is reasonably underexplored relative to their physical relevance quoted above (in para 2). Further, the unsteadiness (time dependency) factor in sandwiched fluid flows makes the problem even more realistic and interesting, which motivated us to consider this problem. To summarise, the practicality and the complexities involved due to the unsteadiness and sandwiched nature of non-Newtonian fluids between Newtonian fluids make the work presented in this paper novel. The solutions of the time-dependent partial differential equations governing the flow are obtained making use of Crank-Nicolson's [23] finite difference approach. The no-slip boundary conditions are applied at the boundaries of the upper and lower plates. In addition, continuity of fluid velocities and shear stresses is assumed at fluid-fluid interfaces.

The paper is organised into five sections. The next section presents the equations associated with the couple stress fluid model followed by mathematical formulation of the problem under consideration, in Cartesian coordinates that govern the flow of immiscible couple stress fluid sandwiched between Newtonian fluids. The initial, boundary and interface conditions are also presented in this section. The finite difference scheme, which gives numerical solutions of the immiscible fluid flow problem considered, is presented in Section 3. Section 4 is dedicated for the discussion of the results, while the conclusions of the current investigation are presented in the last section.

2 Governing Equations and Mathematical Formulation

The equations governing the flow of an incompressible couple stress fluid, in the absence of body couples, are given by [1]

$$\nabla \cdot \bar{q} = 0, \tag{1}$$

$$\rho\left(\frac{\partial \bar{q}}{\partial t} + \bar{q} \cdot \nabla \bar{q}\right) = \rho \bar{F} - \nabla p + \mu \nabla^2 \bar{q} - \eta \nabla^4 \bar{q}, \tag{2}$$

where $\bar{q}$ is the velocity vector, ρ is the density, $\bar{F}$ is the body force per unit mass, μ is the viscosity coefficient and η is the couple stresses viscosity coefficient.

The momentum equation (2) associated to the couple stress fluid model is of higher order than that of the classical Navier-Stokes equations of the Newtonian fluid model. It can be observed that, in absence of couple stresses (i.e. when $\eta = 0$), the momentum equation (2) reduces to

$$\left(\frac{\partial \bar{q}}{\partial t} + \bar{q} \cdot \nabla \bar{q}\right) = \bar{F} - \nabla p + \nabla^2 \bar{q}. \tag{3}$$

Equation (3) is the Navier-Stokes equation of motion for the classical Newtonian fluid model. In view of this, the couple stress fluid model is considered as a simple generalisation of the Newtonian fluid model accounting the couples stresses and body couples in the fluid medium for describing the flow of complex fluids such as animal blood, lubricating oils, liquid crystals, etc.

Consider the unidirectional flow of an immiscible couple stress fluid sandwiched between Newtonian fluids through a horizontal channel. The channel consists of two horizontal parallel plates extending in the X and Z directions, whereas, the Y direction is taken normal to it. The lower and upper plates are situated at $y = -h_1$ and $y = 2h_1$, respectively (see Fig. 1).

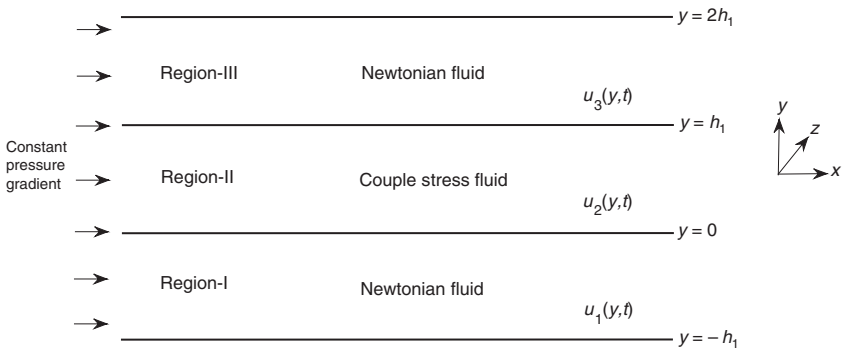

Figure 1: Geometry of the problem.

As the fluids are immiscible, there are three fluid regions: region I ($-h_1 \le y \le 0$) consists of Newtonian fluid of density ρ_1 and viscosity μ_1, region II ($0 \le y \le h_1$) is filled with couple stress fluid of density ρ_2 and viscosity μ_2 and couple stress viscosity coefficient η and region III ($h_1 \le y \le 2h_1$) is filled with the same Newtonian fluid as that of region I. The fluids are assumed to be incompressible, and all the properties of fluids are constant. Under these assumptions, the fluid flow in region II is governed by the differential equations (1) and (2), while the fluid flow in regions I and III is governed by differential equations (1) and (3).

Initially, both plates and the fluids in all the three regions are at rest. At time $t > 0$, a constant pressure gradient is applied in the X direction to generate the flow. Therefore, the velocities in all the fluid regions are taken in the form $\bar{q}_I = (u_I(y, t), 0, 0)$, where $I = 1, 2, 3$. These velocity fields satisfy the incompressibility conditions of the respective flow regions. The momentum equations for the fluid flow, in the absence of body forces and body couples, in all the regions take the form:

Region I ($-h_1 \le y \le 0$) Newtonian fluid region

$$\rho_1 \frac{\partial u_1}{\partial t} = -\frac{\mathrm{d}p}{\mathrm{d}x} + \mu_1 \frac{\partial^2 u_1}{\partial y^2}, \tag{4}$$

Region II ($0 \le y \le h_1$) Couple stress fluid region

$$\rho_2 \frac{\partial u_2}{\partial t} = -\frac{\mathrm{d}p}{\mathrm{d}x} + \mu_2 \frac{\partial^2 u_2}{\partial y^2} - \eta \frac{\partial^4 u_2}{\partial y^4}, \tag{5}$$

Region III ($h_1 \le y \le 2h_1$) Newtonian fluid region

$$\rho_1 \frac{\partial u_3}{\partial t} = -\frac{\mathrm{d}p}{\mathrm{d}x} + \mu_1 \frac{\partial^2 u_3}{\partial y^2}. \tag{6}$$

Because the system is at rest initially, fluids in all the regions have zero velocity for $t \le 0$. Since the plates are stationary in the present case, as a result of the no-slip boundary condition, the fluid velocities at both plates are zero. Because the fluids are immiscible, there are two fluid-fluid interfaces: one at $y = 0$ and the other at $y = h_1$. It is assumed that fluid velocities and shear stresses are continuous at both fluid-fluid interfaces. It should be mentioned here that for the single-fluid flow of the couple stress fluid, in view of the higher-order nature of the momentum equation governing the flow, researchers have been using heuristic boundary conditions proposed by Stokes [2]. However, for the two-fluid flow under consideration, couple stress fluid is sandwiched between Newtonian fluids; there are two fluid-fluid interfaces, each of which has couple stress and Newtonian fluid pair. Therefore, as the stress tensor of the couple stress fluid is not symmetric, continuity assumption of shear stress at each fluid-fluid interface gives two conditions. In view of this, there is no need to consider heuristic boundary conditions.

In mathematical form, these initial, boundary and interface conditions turn out to be:

Initial conditions: for $t \le 0$

$$\begin{aligned} &u_1(y, 0) = 0, \ -h_1 \le y \le 0, \\ &u_2(y, 0) = 0, \ 0 \le y \le h_1, \\ &u_3(y, 0) = 0, \ h_1 \le y \le 2h_1. \end{aligned} \tag{7}$$

Boundary conditions: for $t > 0$

$$\begin{aligned} &u_1(-h_1, t) = 0, \\ &u_3(2h_1, t) = 0. \end{aligned} \tag{8}$$

Interface conditions: for $t > 0$

Continuity of velocities:

$$\begin{aligned} &u_1(0, t) = u_2(0, t), \\ &u_2(h_1, t) = u_3(h_1, t). \end{aligned} \tag{9}$$

Continuity of shear stresses:

$$\mu_1 \frac{\partial u_1}{\partial y} = \mu_2 \frac{\partial u_2}{\partial y} - \eta \frac{\partial^3 u_2}{\partial y^3} \text{ and}$$
$$\mu_1 \frac{\partial u_1}{\partial y} = \mu_2 \frac{\partial u_2}{\partial y} + \eta \frac{\partial^3 u_2}{\partial y^3} \text{ at } y = 0,$$

and

$$\mu_2 \frac{\partial u_2}{\partial y} = \mu_1 \frac{\partial u_3}{\partial y} - \eta \frac{\partial^3 u_2}{\partial y^3} \text{ and}$$
$$\mu_2 \frac{\partial u_2}{\partial y} = \mu_1 \frac{\partial u_3}{\partial y} + \eta \frac{\partial^3 u_2}{\partial y^3} \text{ at } y = h_1,$$

which, after simplification, becomes

$$\mu_1 \frac{\partial u_1}{\partial y} = \mu_2 \frac{\partial u_2}{\partial y} \text{ and } \frac{\partial^3 u_2}{\partial y^3} = 0, \text{ at } y = 0, \tag{10}$$

and

$$\mu_2 \frac{\partial u_2}{\partial y} = \mu_1 \frac{\partial u_3}{\partial y} \text{ and } \frac{\partial^3 u_2}{\partial y^3} = 0 \text{ at } y = h_1. \tag{11}$$

Introducing nondimensional variables,

$$x = h_1 \bar{x},\ y = h_1 \bar{y},\ u_I = U \bar{u}_I,\ t = \frac{h_1 \bar{t}}{U},\ p = \rho_1 U^2 \bar{p}, \tag{12}$$

where $I = 1, 2, 3$,
into the initial boundary value problem (4)–(11), after dropping bars, we get the following:
Region I ($-1 \le y \le 0$) Newtonian fluid region

$$\frac{\partial u_1}{\partial t} = \frac{1}{\mathrm{Re}} \frac{\partial^2 u_1}{\partial y^2} + G, \tag{13}$$

Region II ($0 \le y \le 1$) Couple stress fluid region

$$\frac{\partial u_2}{\partial t} = \frac{m_1}{m_2 \cdot \mathrm{Re}} \frac{\partial^2 u_2}{\partial y^2} - \frac{m_1 \cdot a^2}{m_2 \cdot \mathrm{Re}} \frac{\partial^4 u_2}{\partial y^4} + \frac{G}{m_2}, \tag{14}$$

Region III ($1 \le y \le 2$) Newtonian fluid region

$$\frac{\partial u_3}{\partial t} = \frac{1}{\mathrm{Re}} \frac{\partial^2 u_3}{\partial y^2} + G, \tag{15}$$

Initial conditions: for $t \le 0$

$$\begin{aligned} u_1(y,\ 0) &= 0,\ \ -1 \le y \le 0, \\ u_2(y,\ 0) &= 0,\ \ 0 \le y \le 1, \\ u_3(y,\ 0) &= 0,\ \ 1 \le y \le 2. \end{aligned} \tag{16}$$

Boundary conditions: for $t > 0$

$$\begin{aligned} u_1(-1,\ t) &= 0, \\ u_3(2,\ t) &= 0. \end{aligned} \tag{17}$$

Interface conditions: for $t > 0$
Continuity of velocities:

$$\begin{aligned} u_1(0,\ t) &= u_2(0,\ t), \\ u_2(1,\ t) &= u_3(1,\ t). \end{aligned} \tag{18}$$

Continuity of shear stresses:

$$\frac{\partial u_1}{\partial y} = m_1 \frac{\partial u_2}{\partial y} \text{ and } \frac{\partial^3 u_2}{\partial y^3} = 0, \text{ at } y = 0, \tag{19}$$

$$m_1 \frac{\partial u_2}{\partial y} = \frac{\partial u_3}{\partial y} \text{ and } \frac{\partial^3 u_2}{\partial y^3} = 0, \text{ at } y = 1. \tag{20}$$

where $a = \sqrt{\dfrac{\eta}{h_1^2 \mu_2}}$ is the couple stress parameter, $\mathrm{Re} = \dfrac{\rho_1 U h_1}{\mu_1}$ is the Reynolds number, $G = -\dfrac{\mathrm{d}p}{\mathrm{d}x}$ is the pressure gradient, $m_1 = \dfrac{\mu_2}{\mu_1}$ is the ratio of viscosities and $m_2 = \dfrac{\rho_2}{\rho_1}$ is the ratio of densities.

3 Numerical Solution

The analytical solutions for the current initial boundary value problem (13)–(20) are tedious to find because of the time-dependent nature, the underlying higher-order partial differential equations and the coupled interface conditions. Therefore, a finite difference method is opted to obtain numerical solutions. The domain [–1, 2] is uniformly discretised in space and time considering h and k to be the step sizes in space and time directions, respectively. Following the Crank-Nicolson approach, suitable finite difference approximations for partial derivatives are imposed in all the three regions, as well as on the interfaces. After discretisation, in spatial domain, the lower interface is observed at $i = n$ and the upper interface is at $i = 2n$. The discretised form of the above system (13)–(20) is found to be
Region I: ($i = 1, 2, \ldots, n-1$) Newtonian fluid region

$$\begin{aligned} &-\lambda u_{1i-1,j+1} + (2\lambda + 1) u_{1i,j+1} - \lambda u_{1i+1,j+1} \\ &\quad = \lambda u_{1i-1,j} + (1 - 2\lambda) u_{1i,j} + \lambda u_{1i+1,j} + Gk, \end{aligned} \tag{21}$$

Region II: ($i=n+1,\ n+2,\ \ldots,\ 2n-1$) Couple stress fluid region
for $i=n+1$

$$\begin{aligned} &Ru_{2i-1,j+1}+(Q+O)u_{2i,j+1}+Pu_{2i+1,j+1}\\ &+Bu_{2i+2,j+1}=-Ru_{2i-1,j}-(Q+O)u_{2i,j}\\ &-Pu_{2i+1,j}-Bu_{2i+2,j}+S, \end{aligned} \tag{22}$$

for $i=n+2,\ \ldots,\ 2n-1$

$$\begin{aligned} &Bu_{2i-2,j+1}+Tu_{2i-1,j+1}+(X+2)u_{2i,j+1}\\ &+Tu_{2i+1,j+1}+Bu_{2i+2,j+1}=-Bu_{2i-2,j}\\ &-Tu_{2i-1,j}-(X+2)u_{2i,j}-Tu_{2i+1,j}\\ &-Bu_{2i+2,j}+\frac{2Gk}{m_2}, \end{aligned} \tag{23}$$

Region III: ($i=2n+1,\ 2n+2,\ \ldots,\ 3n-1$) Newtonian fluid region

$$\begin{aligned} &-\lambda u_{3i-1,j+1}+(2\lambda+1)u_{3i,j+1}-\lambda u_{3i+1,j+1}\\ &=\lambda u_{3i-1,j}+(1-2\lambda)u_{3i,j}+\lambda u_{3i+1,j}+Gk. \end{aligned} \tag{24}$$

Discretisation of interface conditions:
for $i=n$

$$u_{1i-1,j+1}-(1+m_1)u_{1i,j+1}+m_1u_{2i+1,j+1}=0, \tag{25}$$

for $i=2n$

$$-m_1u_{2i-1,j+1}+(1+m_1)u_{1i,j+1}-u_{3i+1,j+1}=0, \tag{26}$$

where $\lambda=\dfrac{k}{2\mathrm{Re}\cdot h^2}$, $\alpha=\dfrac{m_1}{m_2\cdot\mathrm{Re}}$, $A=\dfrac{k\alpha}{h^2}$, $B=\dfrac{k\alpha a^2}{h^4}$,
$R=\dfrac{-A^2+2B-6AB-6B^2}{A+2B}$, $Q=\dfrac{2A^2+9AB+6B^2}{A+2B}$,
$O=\dfrac{2A+4B}{A+2B}$, $P=\dfrac{-A^2-6AB-6B^2}{A+2B}$, $S=\dfrac{2Gk(1-B)}{m_2}$,
$T=(-A-4B)$, $X=(2A+6B)$.

The above system of difference equations (21)–(26), when written in matrix form, takes the form

$$WU^{(j+1)}=MU^{(j)}+N,\quad j=0,\ 1,\ 2,\ \ldots \tag{27}$$

where W and M are banded sparse matrices of the order $3n-1$, and N is the column vector of the order $3n-1$ with $n=\dfrac{l}{3}$ and $l=\dfrac{3}{h}$. It is to be mentioned here that l represents the total number of spatial mesh points of [–1, 2]. As the spatial domain [–1, 2] has three uniform parts [–1, 0], [0, 1] and [1, 2] concerning three fluid regions, n represents the number of spatial mesh points in each fluid region.

$U^{(j)}$ is the solution vector at the j^{th} time level, consisting of velocities in all the fluid regions. The expressions for M, N and W are presented in the Appendix A.

The solutions for velocities in each region of flow, as well as at interfaces, can be obtained for every time level by solving the above system (27) for each j.

3.1 Volume Flow Rate

The volume flow rate across the channel in nondimensional form is given by

$$\begin{aligned} Q^*=\int_{-1}^{2}u(y,\,t)\,\mathrm{d}y&=\int_{-1}^{0}u_1(y,\,t)\,\mathrm{d}y+\int_{0}^{1}u_2(y,\,t)\,\mathrm{d}y\\ &+\int_{1}^{2}u_3(y,\,t)\,\mathrm{d}y \end{aligned} \tag{28}$$

As the solutions for fluid velocities are determined numerically, the integration (28) is carried out numerically to obtain the volume flow rate for diverse fluid parameters pertaining to the flow.

4 Discussion of Results

The influence of various fluid parameters such as couple stress parameter, Reynolds number, pressure gradient, ratio of viscosities and ratio of densities on velocity is plotted through Figures 3–8. For plotting the variations, the following set of values are taken: $a=0.5$, $\mathrm{Re}=2$, $G=10$, $m_1=0.5$, $m_2=0.5$, $t=0.5$, $h=0.005$ and $k=0.01$. The choice of step size $h=0.005$ leads to a linear system of the order 601×601 at each time level, which is solved using the Gaussian elimination method.

For the purpose of validation of the present numerical solutions, the acquired numerical results for fluid velocities in the steady-state case and in the absence of couple stresses ($a=0$) are compared with the exact solutions (Appendix B) of Poiseuille flow of Newtonian fluid through a horizontal channel. It is evident from Figure 2 that the present solution is in good agreement with the exact solution.

Figure 3 displays the variation of the velocities with respect to time. It is observed that velocities in all the

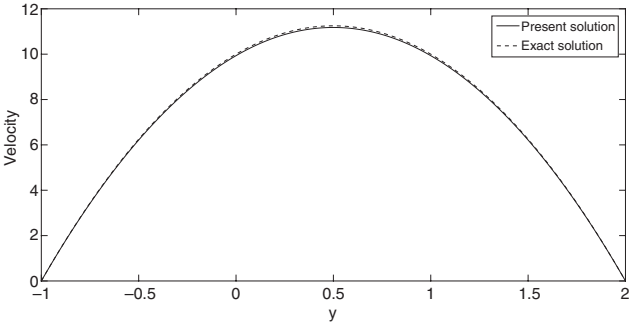

Figure 2: Comparison of the present results with the exact solution.

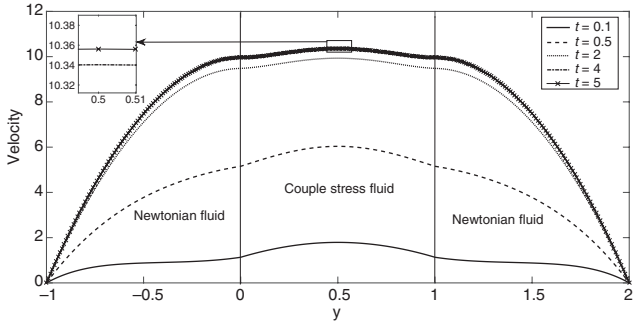

Figure 3: Variations of fluid velocity for various values of t.

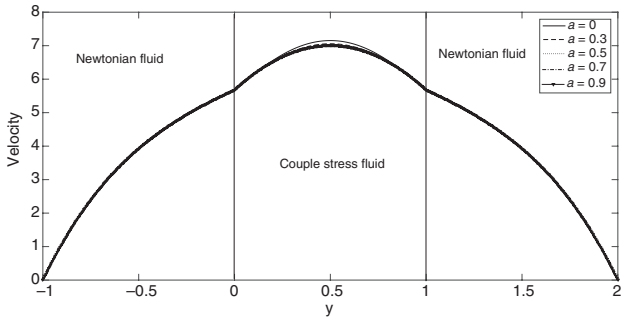

Figure 4: Variations of fluid velocity for various values of a.

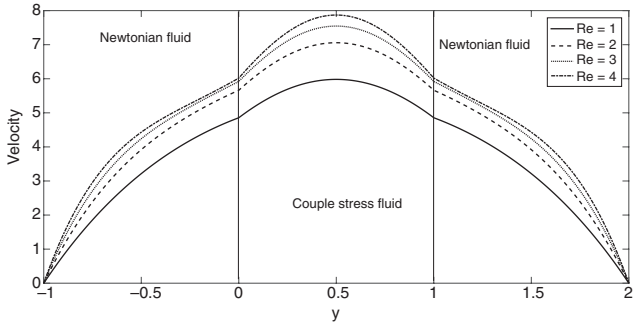

Figure 5: Variations of fluid velocity for various values of Re.

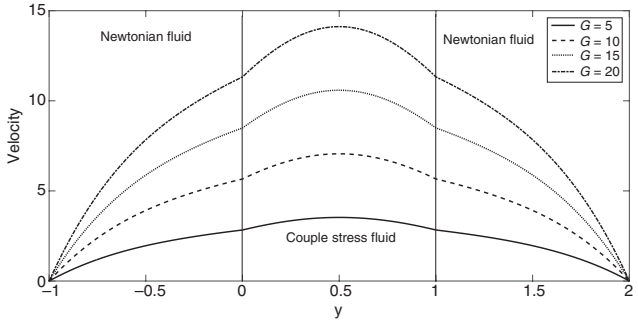

Figure 6: Variations of fluid velocity for various values of G.

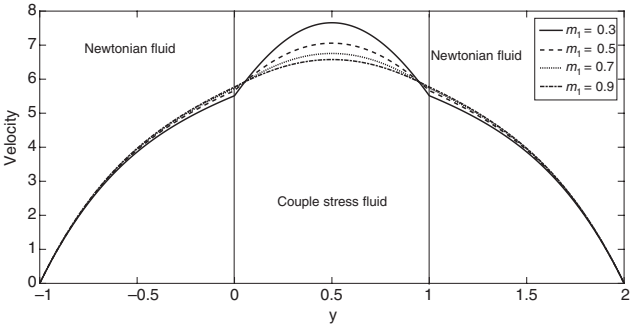

Figure 7: Variations of velocity for various values of m_1.

fluid regions are increasing as time is progressing. After a particular higher value of time, the variation between two consecutive profiles is much less. This means that velocities are reaching a steady state at a higher time level. Figure 4 represents the velocity profile for different values of couple stress parameter a. With the increase of couple stress parameter a, there is a decrease in fluid velocity of region II, while the velocities in region I and region III are almost unchanged. As the couple stresses are present only for the couple stress fluid region, fluid velocity in the couple stress region is decreasing with increment of a, whereas there is no significant change in the fluid velocities in both the Newtonian fluid regions with respect to the couple stress parameter. In the couple stress fluid region, increase in a corresponds to increase in couple stress viscosity coefficient η, which resists the fluid motion. As the value of a is the measure of couple stress effects, when a is made lesser and lesser, the transformation from couple stress fluid to Newtonian fluid takes place; finally, at $a=0$, the profile for Newtonian fluid is obtained.

Figure 5 displays the influence of Reynolds number on velocity profile. Reynolds number Re being $\frac{\rho_1 U h_1}{\mu_1}$, an increase in Re corresponds to a decrease in μ_1. As can be seen from Figure 5, as Reynolds number Re increases,

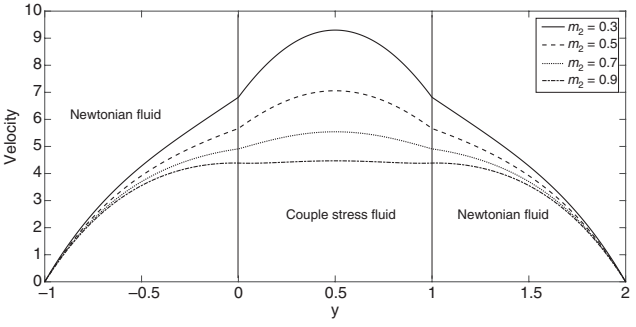

Figure 8: Variations of fluid velocity for various values of m_2.

Table 1: Volume flow rate for various values of G, Re, m_1, m_2 and a.

G	Q^*	Re	Q^*	m_1	Q^*	m_2	Q^*	a	Q^*
5	6.3283	1	10.6640	0.3	12.8480	0.3	15.4273	0.3	12.7169
10	12.6567	2	12.6567	0.5	12.6567	0.5	12.6567	0.5	12.6567
15	18.9850	3	13.5134	0.7	12.5613	0.7	10.8841	0.7	12.6362
20	25.3134	4	14.0227	0.9	12.5052	0.9	9.6639	0.9	12.6272

there is a decrease in viscosity, and thus, the fluid velocity has a tendency to increase. Although Re is defined in terms of ρ_1 and μ_1, in view of the continuity of velocities and shear stresses at the interfaces, there is a transfer of momentum, due to which we have the similar increasing nature of fluid velocities in both the Newtonian fluid regions as well. It is observed that with the increase in Re, velocity increases in all the fluid flow regions. Figure 6 represents the velocity profile for the different values of the pressure gradient. It is observed that with the increase in G, velocity is promoted in all fluid regions. That is, the more the pressure gradient, the more the fluid is pushed to generate the flow, which results in an increase in fluid velocity. Figure 7 shows the nature of velocity profile for different values of m_1. It is seen that the increase in ratio of viscosities m_1 increases the fluid velocities in the Newtonian fluid region and decreases the velocity in the couple stress fluid region. Figure 8 shows the effect of ratio of densities on fluid velocity. It is observed that increase in ratio of densities causes a decrease in fluid velocities in all the three regions.

Table 1 displays the variation of volume flow rate with different fluid parameters. It is noted that volume flow rate is increased by an increase of pressure gradient and Reynolds number and is decreased by an increase of ratio of viscosities, ratio of densities and couple stress parameter.

5 Conclusion

The pressure-driven and time-dependent flow of an immiscible couple stress fluid sandwiched between Newtonian fluids through a horizontal channel has been studied. The governing equations associated with the fluid flow in the respective regions are solved numerically using appropriate initial, boundary and interface conditions. The Crank-Nicolson finite difference approach has been used to obtain numerical solutions.

The main findings of the current study are summarised as follows:

(i) Fluid velocities in all the regions are increasing with time. After a certain higher time level onwards, velocities enter into a steady state.

(ii) Fluid velocity in the couple stress fluid region is suppressed by the supplement of the couple stress parameter. The couple stress parameter has no significant influence on the Newtonian fluid regions.

(iii) Increase of Reynolds number promote the fluid velocities in all the three regions comprehensively.

(iv) An increasing nature is noted in the velocities of both Newtonian fluid regions, when varied with ratio of viscosities. Whereas velocity decreases with an increase of viscosity ratio in the couple stress fluid region.

(v) Volume flow rate is enhanced by an increase of Reynolds number and suppressed by the increase of the couple stress parameter.

Nomenclature

a	couple stress fluid parameter
$\bar{F}$	body force vector
G	constant pressure gradient
h	spatial step size
h_1	width of each region
(i, j)	discretisation parameters
k	temporal step size
m_1	ratio of viscosities
m_2	ratio of densities
$n, 2n$	interfaces
p	fluid pressure
$\bar{q}$	fluid velocity vector
Q^*	volume flow rate
Re	Reynolds number
t	time
u_1	component of fluid velocities in region I
u_2	component of fluid velocities in region II
u_3	component of fluid velocities in region III
U	average fluid velocity in channel
(x, y, z)	Cartesian coordinate system
η	couple stress viscosity coefficient
μ	viscosity of the fluid
μ_1	viscosity of fluids in region I and region III
μ_2	viscosity of fluid in region II
ρ	density of the fluid
ρ_1	density of fluids in region I and region III
ρ_2	density of fluid in region II

Acknowledgments: The authors thank the reviewers for their suggestions, which led to the strengthening of the paper.

Appendix A

$W=(w_{ij})_{(3n-1)\times(3n-1)}$, $M=(m_{ij})_{(3n-1)\times(3n-1)}$ and $N=(n_j)_{(3n-1)\times 1}$, where,

$$w_{ij}=\begin{cases}0, & \text{for } i+2<j\\ \Omega_{1i}, & \text{for } i+2=j\\ \beta_{1i}, & \text{for } i+1=j\\ \alpha_{1i}, & \text{for } i=j\\ \gamma_{1i}, & \text{for } i=j+1\\ \delta_{1i}, & \text{for } i=j+2\\ 0, & \text{for } i<j+2,\end{cases}$$

$$m_{ij}=\begin{cases}0, & \text{for } i+2<j\\ \Omega_{2i}, & \text{for } i+2=j\\ \beta_{2i}, & \text{for } i+1=j\\ \alpha_{2i}, & \text{for } i=j\\ \gamma_{2i}, & \text{for } i=j+1\\ \delta_{2i}, & \text{for } i=j+2\\ 0, & \text{for } i<j+2,\end{cases}$$

and

$$n_j=\begin{cases}kG, & \text{for } j=1 \text{ to } n-1\\ 0, & \text{for } j=n \text{ and } 2n\\ \dfrac{2kG}{m_2} & \text{for } j=n+1 \text{ to } 2n-1\\ kG, & \text{for } j=2n+1 \text{ to } 3n-1.\end{cases}$$

In the above,

$$\alpha_{1i}=\begin{cases}(1+2\lambda), & \text{for } i=1 \text{ to } n-1\\ -(1+m_1), & \text{for } i=n\\ Q+O, & \text{for } i=n+1 \text{ and } i=2n-1\\ 2(A+3B+1), & \text{for } i=n+2 \text{ to } 2n-2\\ (1+m_1), & \text{for } i=2n\\ (1+2\lambda), & \text{for } i=2n+1 \text{ to } 3n-1,\end{cases}$$

$$\beta_{1i}=\begin{cases}-\lambda, & \text{for } i=2 \text{ to } n-1\\ 1, & \text{for } i=n\\ R, & \text{for } i=n+1\\ T, & \text{for } i=n+2 \text{ to } 2n-2\\ P, & \text{for } i=2n-1\\ -m_1, & \text{for } i=2n\\ -\lambda, & \text{for } i=2n+1 \text{ to } 3n-1,\end{cases}$$

$$\gamma_{1i}=\begin{cases}-\lambda, & \text{for } i=1 \text{ to } n-1\\ m_1, & \text{for } i=n\\ P, & \text{for } i=n+1\\ T, & \text{for } i=n+2 \text{ to } 2n-2\\ R, & \text{for } i=2n-1\\ -1, & \text{for } i=2n\\ -\lambda, & \text{for } i=2n+1 \text{ to } 3n-2,\end{cases}$$

$$\Omega_{1i}=\begin{cases}B, & \text{for } i=n+2 \text{ to } 2n-1\\ 0, & \text{otherwise,}\end{cases}$$

$$\delta_{1i}=\begin{cases}B, & \text{for } i=n+1 \text{ to } 2n-2\\ 0, & \text{otherwise,}\end{cases}$$

$$\alpha_{2i}=\begin{cases}(1-2\lambda), & \text{for } i=1 \text{ to } n-1\\ 0, & \text{for } i=n\\ -(Q+O), & \text{for } i=n+1\\ F, & \text{for } i=n+2 \text{ and } i=2n-2\\ -(Q+O), & \text{for } i=2n-1\\ 0, & \text{for } i=2n\\ (1-2\lambda), & \text{for } i=2n+1 \text{ to } 3n-1,\end{cases}$$

$$\beta_{2i}=\begin{cases}\lambda, & \text{for } i=2 \text{ to } n-1\\ 0, & \text{for } i=n\\ -R, & \text{for } i=n+1\\ -T, & \text{for } i=n+2 \text{ to } 2n-2\\ -P, & \text{for } i=2n-1\\ 0, & \text{for } i=2n\\ \lambda, & \text{for } i=2n+1 \text{ to } 3n-1,\end{cases}$$

$$\gamma_{2i}=\begin{cases}\lambda, & \text{for } i=1 \text{ to } n-1\\ 0, & \text{for } i=n\\ -P, & \text{for } i=n+1\\ -T, & \text{for } i=n+2 \text{ to } 2n-2\\ -R, & \text{for } i=2n-1\\ 0, & \text{for } i=2n\\ \lambda, & \text{for } i=2n+1 \text{ to } 3n-2,\end{cases}$$

$$\Omega_{2i}=\begin{cases}-B, & \text{for } i=n+2 \text{ to } 2n-1\\ 0, & \text{otherwise,}\end{cases}$$

$$\delta_{2i}=\begin{cases}-B, & \text{for } i=n+1 \text{ to } 2n-2\\ 0, & \text{otherwise.}\end{cases}$$

Appendix B

For the purpose of comparison, consider the flow of the same Newtonian fluid through a horizontal channel (see Fig. 1) in all the three regions. The governing equation (3) for the steady flow of Newtonian fluid through the horizontal channel reduces to

$$-\frac{\mathrm{d}p}{\mathrm{d}x}+\mu\frac{\mathrm{d}^2u}{\mathrm{d}y^2}=0, \tag{B.1}$$

with the boundary conditions,

$$\begin{aligned} &u(y)=0 \text{ at } y=-h_1 \text{ and}\\ &u(y)=0 \text{ at } y=2h_1. \end{aligned} \tag{B.2}$$

Using the non-dimensional scheme (12), the equations (B.1) and (B.2) become

$$\frac{\mathrm{d}^2u}{\mathrm{d}y^2}+\mathrm{Re}G=0, \tag{B.3}$$

with

$$\begin{aligned} &u(y)=0 \text{ at } y=-1 \text{ and}\\ &u(y)=0 \text{ at } y=2. \end{aligned} \tag{B.4}$$

Solving the ODE (B.3) with the prescribed conditions (B.4), the exact solution is obtained as

$$u(y)=\frac{\mathrm{Re}G}{2}[2+y-y^2]. \tag{B.5}$$

This velocity field for the Newtonian fluid case has been used to compare the results of limiting solutions of the sandwiched flow problem studied in this paper.

References

[1] V. K. Stokes, Phys. Fluids **9**, 1709 (1966).
[2] V. K. Stokes, Theories of Fluids With Microstructure – An Introduction, Springer-Verlag, New York 1984.
[3] N. B. Naduvinamani, P. S. Hiremath, and G. Gurubasavaraj, Tribol. Int. **34**, 739 (2001).
[4] N. B. Naduvinamani, P. S. Hiremath, and G. Gurubasavaraj, Fluid Dyn. Res. **31**, 333 (2002).
[5] P. Chaturani, Biorheology **15**, 119 (1978).
[6] M. Devakar and T. K. V. Iyengar, Nonlinear Anal. Model. **15**, 29 (2010).
[7] S. Maiti and J. C. Misra, J. Mech. Med. Biol. **12**, 1250048 (2012).
[8] T. Hayat, Z. Iqbal, M. Qasim, and O. M. Aldossary, Z. Naturforsch. A **67**, 217 (2012).
[9] M. Devakar, D. Sreenivasu, and B. Shankar, Alexandria Eng. J. **53**, 723 (2014).
[10] Z. Abbas, J. Hasnain, and M. Sajid, Z. Naturforsch. A **69**, 553 (2015).
[11] S. Asad, A. Alsaedi, and T. Hayat, Appl. Math. Mech. Engl. Ed. **37**, 315 (2016).
[12] N. B. Naduvinamani, S. T. Fathima, and P. S. Hiremath, Tribol. Int. **36**, 949 (2003).
[13] N. B. Naduvinamani, P. S. Hiremath, and G. Gurubasavaraj, Tribol. Int. **38**, 451 (2005).
[14] J. R. Lin and C. R. Hung, Fluid Dyn. Res. **39**, 616 (2007).
[15] J. R. Lin, L. M. Chu, C. R. Hung, and R. F. Lu, Z. Naturforsch. A **66**, 512 (2014).
[16] P. Chaturani and R. P. Samy, Biorheology **22**, 521 (1985).
[17] K. Haldar and H. I. Anderson, Acta Mech. **117**, 221 (1996).
[18] H. L.Goldsmith and R. Skalak, Annual Review of Fluid Dynamics, Annual Review Inc., Palo Alto, CA 1975, p. 231.
[19] J. C. Umavathi, A. J. Chamkha, M. H. Manjula, and A. Al-Mudhaf, Can. J. Phys. **83**, 705 (2005).
[20] J. C. Umavathi, J. Prathap Kumar, and A. J. Chamkha, Can. J. Phys. **86**, 961 (2008).
[21] J. C. Umavathi, Heat Transf. Asian Res. **41**, 444 (2012).
[22] J. C. Umavathi, I. C. Liu, J. Prathap-Kumar, and D. Shaikh-Meera, Appl. Math. Mech. Engl. Ed. **31**, 1497 (2010).
[23] J. Crank and P. Nicolson, Proc. Camb. Phil. Soc. **43**, 50 (1947).